# Pre-engineered abruptly autofocusing beams

**Ioannis Chremmos,[1,*] Nikolaos K. Efremidis,[2] and Demetrios N. Christodoulides[3]**

[1]*Archimedes Center for Modeling, Analysis and Computation (ACMAC), Department of Applied Mathematics, University of Crete, Heraklion 71409, Crete, Greece*

[2]*Department of Applied Mathematics, University of Crete, Heraklion 71409, Crete, Greece*

[3]*CREOL/College of Optics, University of Central Florida, Orlando, Florida 32816, USA*

**Corresponding author: jochremm@central.ntua.gr*

Received March 21, 2011; accepted April 15, 2011;
posted April 15, 2011 (Doc. ID 144506); published May 13, 2011

We introduce a new family of $(2+1)D$ light beams with pre-engineered abruptly autofocusing properties. These beams have a circularly symmetric input profile that develops outward of a dark disk and oscillates radially as a sublinear-chirp signal, creating a series of concentric intensity rings with gradually decreasing width. The light rays involved in this process form a caustic surface of revolution that bends toward the beam axis at an acceleration rate that is determined by the radial chirp itself. The collapse of the caustic on the axis leads to a large intensity buildup right before the intended focus. This ray-optics interpretation provides valuable insight into the dynamics of abruptly autofocusing waves. 

*OCIS codes:* 050.1940, 260.2030, 350.5500.

Recently, a new class of light beams has been revealed with abruptly autofocusing (AAF) properties [1]. As opposed to self-focusing effects mediated by Kerr nonlinearities, this autofocusing behavior is purely linear in origin and is a result of the optical field structure itself. During propagation, these AAF fields can maintain a relatively low intensity profile while suddenly releasing all their energy right before a target. The first AAF beam proposed [1] exhibited a $(2+1)D$ circularly symmetric field that involved the salient diffraction-resisting and self-bending features of a finite-energy $(1+1)D$ Airy beam [2,3]. As the Airy radial profile is accelerated toward the center, a paraboloid caustic surface is formed that "collapses" on axis—thus leading to a large intensity buildup right before the intended focus. The intensity contrast reached at the focus compared to the maximum input intensity was shown to reach several orders of magnitude. Moreover, due to the diffraction-free character of $(1+1)D$ Airy beams, the maximum intensity of the wave over the transverse plane remains almost constant along the entire propagation path until the focus is reached. As indicated in [1], AAF waves may prove advantageous in medical laser treatments and in other nonlinear optical settings over standard Gaussian beams obeying a more gradual Lorentzian focusing law.

In this Letter, we report on a new family of AAF beams. These are circularly symmetric waves whose input amplitude develops outward of a dark disk and oscillates radially as a sublinear chirp signal. During propagation, these wavefronts form inward-bending caustic surfaces of revolution with an acceleration that is directly related to their chirp rate. We hereby extend the family of circular Airy beams [1], the rays of which are known to form paraboloids as a result of the quadratic inward radial shift of the Airy rings. This new flexibility comes at the cost of losing the unique diffraction-resisting properties of the Airy waveform, which is, however, here traded for greater transverse accelerations, enhanced focusing abruptness, and larger intensity contrasts.

We begin with the scaled paraxial equation of light in cylindrical coordinates $(r,\varphi,z)$

$$2iu_z + u_{rr} + r^{-1}u_r + r^{-2}u_{\varphi\varphi} = 0, \tag{1}$$

where the radial distance $r$ is normalized with respect to an arbitrary transverse length $x_0$ and the propagation distance $z$ is normalized with $kx_0^2$, $k$ being the wavenumber. The proposed beams are solutions of Eq. (1) with an azimuth-independent initial condition

$$u(r,z=0) = A(r)\sin[q(r)], \tag{2}$$

where $A$ is an envelope function, such that the total conveyed power $2\pi\int_0^\infty |u|^2 r\mathrm{d}r$ is finite, and $q$ is the phase of a sublinear chirp signal

$$q(r) = \begin{cases} C(r-r_0)^\beta, & r \geq r_0 \\ 0, & r < r_0 \end{cases}, \tag{3}$$

where $C>0$ and $1<\beta<2$. The term sublinear stems from the fact that the phase of a linear chirp is quadratic ($\beta=2$). In what follows, we will see that the sublinearity of the chirp rate is a prerequisite for the AAF phenomenon. From Eq. (2), it is also obvious that, since $u(r\leq r_0)=0$ (a dark disk), only $A(r>r_0)$ needs to be defined. For any given input amplitude, the solution to Eq. (1) can be written in terms of the Fresnel integral

$$u(r,\varphi,z) = \int_0^{2\pi}\int_0^\infty \frac{u(\rho,\theta,0)}{2\pi iz} e^{i\frac{\rho^2+r^2-2\rho r\cos(\varphi-\theta)}{2z}}\rho\mathrm{d}\rho\mathrm{d}\theta. \tag{4}$$

Being in the paraxial regime, the wave dynamics can be efficiently described by a ray-optics picture that follows from a stationary phase computation of this integral. An application of this same concept to the $(1+1)D$ Airy beam was done in [4], while a geometric optics perspective was also presented in [5]. Substituting $u(\rho,\theta,0)$ from Eq. (2), with $\sin(q)=[\exp(iq)-\exp(-iq)]/2i$, one arrives at the conclusion that the wave in the region $r<r_0$ and near or above the caustic surface results from the interference of the inward light rays that are due to term $\exp(-iq)$ only. These are expressed by the stationary phase conditions $\theta=\varphi$ and $q'(\rho)=(\rho-r)/z$, where $q'(\rho)\equiv dq/d\rho$. Such a ray emerges from point $(\rho,\theta)$ on the input plane and propagates along the plane $\varphi=\theta$ at an

 

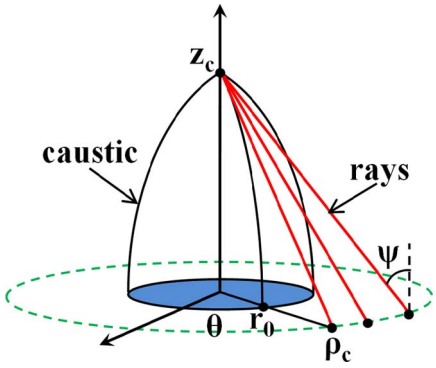


Fig. 1. (Color online) Ray-optics schematic: The rays emerging from the circle with radius $\rho_c$ meet on axis at $z = z_c$, exactly where the caustic surface collapses.

inward angle $\psi(\rho) = \tan^{-1}(q')$ with the $z$ axis (Fig. 1). The continuum of rays emerging from points with a common azimuth, i.e., $(\rho, \theta)$, $\rho \geq r_0$, form a caustic curve that is parametrically expressed as $(r, \varphi, z) = (\rho - q'/q'', \theta, 1/q'')$, where $\rho \geq r_0$ is the parameter. The continuum of these caustics for $0 \leq \theta < 2\pi$ forms a caustic surface of revolution, which may be conveniently expressed as

$$r = r_0 - \frac{[C\beta(\beta-1)z]^{\nu}}{\nu - 1}, \tag{5}$$

where $\nu = (2-\beta)^{-1}$. It turns out that the chirp parameter $\beta$ determines the order $\nu$ of the caustic, and also that the condition $1 < \beta < 2$ (sublinear chirp) ensures $\nu > 1$, i.e., that the caustic is bent with acceleration toward the axis. For example, if $C = 2/3$ and $\beta = 3/2$, one obtains the caustic $(r_0 - z^2/4, z)$, whose generating curve is the same as the familiar parabolic trajectory of $(1+1)D$ Airy beams $(x = z^2/4)$. Indeed, by recalling the asymptotic expression $\mathrm{Ai}(-x) \sim \sin[(2/3)x^{3/2} + \pi/4]/\sqrt{\pi}x^{1/4}$, one sees that the circular Airy beam of [1] can be approximately considered as a beam of the family of Eq. (2) with the above chirp parameters.

Through the ray-optics approach, one also finds that the wave at an arbitrary point $(r, \varphi, z)$ in the considered region results from the interference of two rays emerging from points $(\rho_{1,2}, \varphi, 0)$, where $\rho_{1,2}$ are the two solutions of $q' = (\rho - r)/z$. For points lying on the caustic surface, Eq. (5), the two first-order stationary points collapse to a second-order one [6]. The maximum amplitude gradient occurs at $(r = 0, z_c)$ where the caustic surface meets the axis, and $z_c$ is obtained from Eq. (5) for $r = 0$. The wave at this point is due to the constructive interference of the continuum of rays emerging from the circle $(\rho_c, \varphi, 0)$, $0 \leq \varphi < 2\pi$, where $\rho_c = \nu r_0$. Using a second-order stationary phase method [6], it can be shown that the wave amplitude at this point is

$$u(r = 0, z_c) \simeq \frac{\pi \rho_c A(\rho_c)\mathrm{Ai}(0)}{z_c[-q'''(\rho_c)/2]^{1/3}} e^{i[\rho_c^2/2z_c - q(\rho_c)]}. \tag{6}$$

The latter is also valid approximately for on-axis points $(0, z)$ in the neighborhood of $(0, z_c)$, however, with $\mathrm{Ai}(0)$ replaced by $\mathrm{Ai}(-\sigma)$ where $\sigma \approx \sigma'(z_c)(z - z_c)$ and $\sigma'(z_c) = \rho_c z_c^{-2}[-q'''(\rho_c)/2]^{-1/3}$. Recalling the shape of the Airy function, we deduce that $(0, z_c)$ is a point of maximum amplitude gradient $(\mathrm{Ai}''(0) = 0)$ and that the focal point $(0, z_f)$ occurs approximately when $\sigma \approx 1$, hence

$$z_f \approx z_c + \frac{1}{\sigma'(z_c)} = \frac{[(\nu-1)r_0]^{1/\nu}}{C\beta(\beta-1)} + \frac{1}{\sigma'(z_c)}. \tag{7}$$

The factor $A(\rho_c)$ in Eq. (6) implies that the wave amplitude near the focus is determined mainly by the values of the input wavefront on the circle $\rho = \rho_c$, chirp parameters $C, \beta$ being fixed. This is an important general conclusion for engineering AAF waves: The larger the acceleration (or the order $\nu$) of the caustic surface, the greater has to be the radial extent (at least $\nu r_0$) of the input wavefront in order to sustain the abrupt focusing. Equation (6) also reveals the dependence of focusing on $q'''$.

Let us now examine a few examples pertaining to some of the properties of these beams. The evolution of the waves is numerically computed using the Hankel transform method [1]. In our numerical investigations, the parameter $C$ is scaled out by setting $C = \pi$, which is equivalent to the second zero of the input profile occurring at the radius $r = r_0 + 1$. The input radial profile of a beam with $\beta = 3/2$ and exponential envelope $A(r) = \exp[a(r_0 - r)]$ is shown in Fig. 2(a) when $a = 0.2$ and $r_0 = 4$, while Fig. 2(b) shows the evolution of its intensity in space. As predicted by the analysis, a paraboloid caustic is formed that collapses on the axis at $z_c \approx 0.85$ where the amplitude gradient is maximum. The focus occurs right after, at $z_f \approx 0.881$, which agrees well with the value 0.887 predicted by Eq. (7). Figure 2(c) shows the maximum intensity versus the propagation distance with normalized $I_{\max}(0) = 1$, clearly verifying the AAF phenomenon that starts at $z \approx 0.79$ with a contrast ~7 to exceed 300 on focus. The analytically predicted contrast is remarkably close: 295. The abruptness of the focusing can be appreciated by assuming the $I_{\max}(z)$ curve of a Gaussian beam that achieves the same contrast $I_0$ at the same focal distance $z_f$, i.e., $I_{\max}(z) = I_0[1 + (I_0 - 1)(z/z_f - 1)^2]^{-1}$. The Lorentzian curve focuses much more slowly.

We now assume a beam with faster input oscillations, so that $\beta = 5/3$, and the same exponential amplitude, hence having approximately the same total power as the beam of Fig. 1. The AAF phenomenon of this beam is illustrated in Fig. 3. The formed caustic is now of cubic

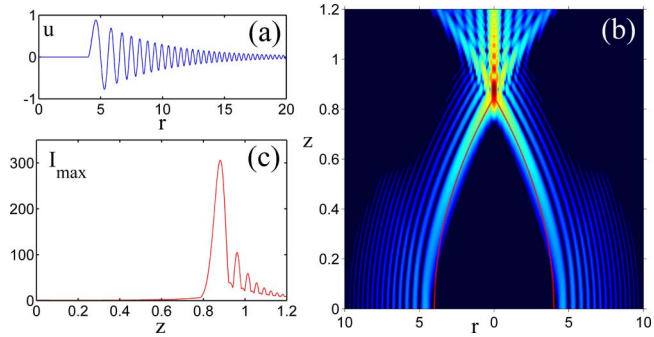


Fig. 2. (Color online) (a) Radial input amplitude, (b) intensity evolution (in logarithimic scale), and (c) intensity contrast versus propagation distance for a beam with $C = \pi$, $\beta = 3/2$, $r_0 = 4$, and $A(r) = \exp[0.2(4 - r)]$. The red detail in (b) is the paraboloid caustic of Eq. (5).

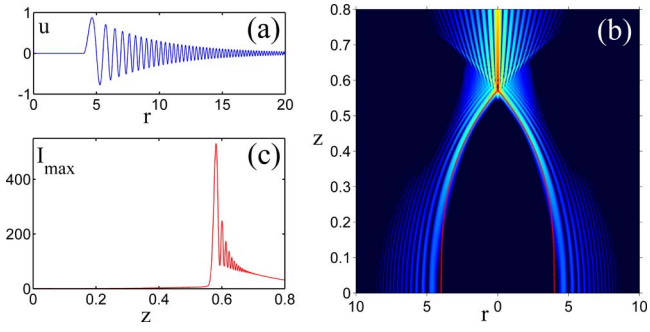


Fig. 3. (Color online) Similar to Fig. 2 but with $\beta = 5/3$.

order ($\nu = 3$), hence the focus occurs at a shorter distance $z_f \approx 0.581$, which agrees well with the value 0.582 predicted by Eq. (7). As seen from Fig. 2(c), the focusing is now more abrupt, with an intensity that starts increasing from around 11 at $z \approx 0.557$ to above 530 at the focus. The predicted value is 520.

The enhanced abruptness and contrast of AAF in a beam with higher $\beta$ comes at the cost of increased sensitivity of this contrast to the radius $r_0$ of the input dark disk. This is shown in Fig. 4, where $I_{\max}$ is given versus $r_0$ for the two considered beams. Although it reaches higher values, the peak contrast of the beam with the faster chirp-rate drops (and increases) faster with $r_0$. This can be intuitively explained through Eq. (6): The rays that interfere to produce the wave around the focal region stem from input circumferences with radii around $\rho_c = \nu r_0$. Therefore, with a given $A(r)$, a higher $\nu$ implies weaker rays and a contrast that drops faster with $r_0$. Equation (6) also accounts for the values of $I_{\max}$, since a higher $\nu$ implies a higher $\rho_c$, and lower $z_c$, $q'''$. Higher intensity contrasts are also obtained with lower apodization rates $a$, i.e., slower decreasing envelope functions.

In addition to the chirp-rate, the envelope of the input amplitude can also be engineered to produce various AAF beams. For example, since the rays responsible for the formation of the caustic surface and the focal spot originate from an input annulus $r_0 \le r \le \rho_{\max}$, where $\rho_{\max} > \rho_c$, one can define $A(r)$ to be nonzero only within

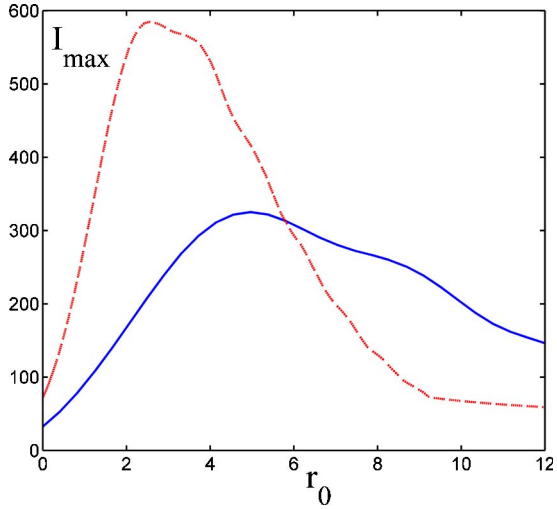


Fig. 4. (Color online) Maximum intensity contrast versus $r_0$ for the beams of Fig. 2 (solid blue curve) and Fig. 3 (dashed red curve).

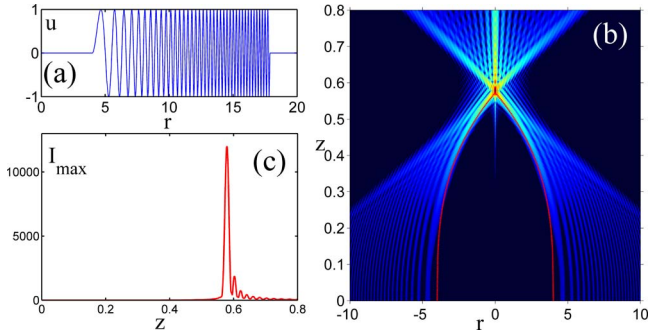


Fig. 5. (Color online) Similar to Fig. 3 with an envelope function $A(r) = 1$ for $4 \le r \le 4 + 80^{3/5}$ and zero elsewhere.

this annulus. In this way, one obtains higher intensity contrasts because the interfering rays are of equal initial amplitude, as well as suppressed secondary on-axis maxima. Figure 5 shows the dynamics of such a beam with $\beta = 5/3$, $C = \pi$, $r_0 = 4$, and $\rho_{\max} = r_0 + 80^{3/5}$, the latter value being selected to allow exactly 40 oscillations of the input radial profile, as shown in Fig. 5(a). In Fig. 5(c), the intensity contrast now reaches 12000 on-focus and the second maximum is ~8 dB lower, which should be compared to approximately 3.2 dB of Fig. 3(c).

The key concept behind the introduced beams, viz. the radial chirp of the input amplitude, can be utilized to design an endless variety of AAF beams. For example, the basic definition of Eq. (2) can be expanded to beams with a $\cos q$ or $\exp(-iq)$ input profile. One could also assume linear superpositions of beams with different parameters $\beta$ and/or $r_0$ that are selected so that their caustic surfaces collapse at the same on-axis point.

In conclusion, we have significantly expanded the recently introduced family of AAF waves. By virtue of the chirped radial oscillations of their input amplitude, the new members can abruptly focus their power after writing caustic surfaces of revolution of any desired order. There are 2 degrees of freedom in pre-engineering the AAF process: the radial chirp rate, which determines the shape of the caustic, and the envelope profile, which can be designed to increase the contrast and tailor the shape of the focusing spot. Beams with higher chirp rates are in general appropriate for enhanced abruptness and greater intensity contrasts, however, at shorter focal distances.

This work was supported in part by the Archimedes Center for Modeling, Analysis and Computation (ACMAC) (project FP7-REGPOT-2009-1) and the United States Air Force Office of Scientific Research (USAFOSR) (grant no. FA9550-10-1-0561).

**References**

1. N. Efremidis and D. Christodoulides, Opt. Lett. **35**, 4045 (2010).
2. G. Siviloglou and D. Christodoulides, Opt. Lett. **32**, 979 (2007).
3. G. Siviloglou, J. Broky, A. Dogariu, and D. Christodoulides, Phys. Rev. Lett. **99**, 213901 (2007).
4. Y. Kaganovsky and E. Heyman, Opt. Express **18**, 8440 (2010).
5. S. Vo, K. Fuerschbach, K. Thompson, M. Alonso, and J. Rolland, J. Opt. Soc. Am. A **27**, 2574 (2010).
6. L. Felsen and N. Marcuvitz, *Radiation and Scattering of Waves* (Wiley-IEEE, 1994).